Malaysian Journal of Analytical Sciences, Vol 26 No 5 (2022): 1023 - 1036

Malaysian Journal of Analytical Sciences (MJAS)
Published by Malaysian Analytical Sciences Society

BIOTEMPLATED BISMUTH FERRITE ($BiFeO_3$) NANOCATALYST FOR THE PHOTODEGRADATION OF OFLOXACIN BY SOLAR LIGHT UNDER THE INFLUENCE OF OPERATIONAL PARAMETERS

(Templat Bio Bismut Ferit ($BiFeO_3$) Nanopemangkin untuk Fotodegradasi Ofloxacin Menggunakan Cahaya Suria Dibawah Pengaruh Parameter Operasi)

Ahmad Fadhil Rithwan[1], Muhammad Alif Abdul Khani[1], Noor Haida Mohd Kaus[1]*, Rohana Adnan[1], Sirikanjana Thongmee[2], Siti Fairus Mohd Yusoff[3], Takaomi Kobayashi[4], Mohd Amirul Ramlan[5]

[1] School of Chemical Sciences,
Universiti Sains Malaysia, 11800, Pulau Pinang, Malaysia
[2]Physics Department,
Faculty of Science, Kasetsart University, Bangkok 10900, Thailand
[3] Department of Chemical Sciences,
Faculty of Science and Technology, Universiti Kebangsaan Malaysia,
Bangi 43600, Selangor, Malaysia
[4]Department of Materials Science and Technology,
Nagaoka University of Technology Nagaoka, Japan
[5]Department of Polytechnic & Community Colleges Education,
Ministry of Higher Education, Persiaran Perdana, Presint 4, Putrajaya 62100, Malaysia

**Corresponding author: noorhaida@usm.my*

Received: 2 March 2022; Accepted: 3 July 2022; Published: 30 October2022

Abstract

Bismuth ferrite ($BiFeO_3$) has been demonstrated to be one of the most efficient perovskite-based photocatalysts for pollutant degradation under direct sunlight. The focus of this research was to study the photocatalytic activity of $BiFeO_3$ in relation to the degradation of the antibiotic ofloxacin. Different operational parameters for the optimized system were determined, such as photocatalyst dosage (0.05 g L^{-1} to 0.50 g L^{-1}), pollutant concentration (2.5 mg L^{-1} to 20 mg L^{-1}), reaction duration (2 hours), pH of solution (pH 2 to pH 12), and the effect of hydrogen peroxide, H_2O_2 as an oxidant (0.1 M to 0.7 M). X-ray Diffraction (XRD), Scanning Electron Microscope-Energy Dispersive X-ray (SEM-EDX), and Fourier Transform Infrared Spectroscopy (FTIR) analyses all corroborated that the rhombohedral $BiFeO_3$ has a high purity and large surface area. The most efficient condition for all selected parameters was 0.07 g L^{-1} $BiFeO_3$ at pH 8 in 10 mg L^{-1} of ofloxacin and the addition of 0.3 M H_2O_2 with 70.1% degradation and the total organic carbon left in the solution was 9.36%. The reaction obeyed pseudo-first order kinetics with R^2 value obtained is 0.9399, with decreasing k values as the initial concentration increased. This demonstrated that the system performed best at low concentrations. This discovery paves the way for future research into the operational parameters that contribute to the photocatalyst efficacy in removing antibiotics as a pollutant.

Keywords: photocatalysis, photofunctional material, ofloxacin, visible light source, bismuth ferrite

Abstrak

Ferit bismut, $BiFeO_3$ terbukti sebagai salah satu daripada fotopemangkin berasaskan perovskit terbaik untuk degradasi pelbagai pencemar di bawah cahaya matahari langsung. Kajian ini dijalankan untuk mempelajari prestasi fotoaktiviti $BiFeO_3$ terhadap degradasi antibiotik ofloxacin. Parameter operasi yang berbeza telah ditentukan untuk sistem yang dioptimumkan termasuk dos fotopemangkin (0.05 g L^{-1} hingga 0.50 g L^{-1}), kepekatan bahan cemar (2.5 mg L^{-1} hingga 20 mg L^{-1}), masa tindak balas (2 jam), pH (pH 2 hingga pH 12), dan kesan hidrogen peroksida (H_2O_2) sebagai agen pengoksidaan (0.1 M hingga 0.7 M). Keputusan analisis pembelauan sinar-x (XRD), spektroskopi inframerah-transformasi Fourier (FT-IR) dan mikroskop elektron imbasan-spektroskopi sinar-x penyebaran tenaga (SEM-EDX) mengesahkan ketulenan tinggi $BiFeO_3$ rombohedral yang telah dihasilkan dengan luas permukaan yang tinggi. Keadaan yang paling berkesan untuk semua parameter terpilih adalah dos $BiFeO_3$ 0.07 g L^{-1} pada pH 8 di dalam 10 mg L^{-1} ofloxacin dengan penambahan 0.3 M H_2O_2 yang menghasilkan degradasi ofloxacin sebanyak 70.1% dan jumlah kesuluruhan karbon yang tinggal didalam larutan adalah sebanyak 9.36 %. Tindak balas ini tergolong di dalam urutan kinetik pseudo-pertama dengan nilai R^2 tercapai sebanyak 0.9399, dengan nilai *k* menurun apabila kepekatan awal meningkat. Ini menunjukkan bahawa sistem ini adalah lebih efisyen pada kepekatan yang rendah. Penemuan ini telah membuka satu kajian berpotensi ke arah penerokaan faktor yang meningkatkan kecekapan fotopemangkin bagi penyingkiran pencemar antibiotik.

Kata kunci: fotopemangkinan, bahan fotofungsian, ofloxacin, sumber cahaya boleh lihat, bismut ferit

Introduction

Urbanization and industrialization have a detrimental effect on many countries water sources. Textile industries, hospitals, farms, and residences may discharge a variety of contaminants, including dyes [1], heavy metals [2], pesticides [3], and antibiotics [4]. Antibiotics can be classified as an emerging contaminant since their concentration in water bodies has increased over the years due to increases in utilization rates in the human and livestock sectors [5]. According to Ambrosetti et al. [6], antibiotics may exist in the environment as parent molecules, breakdown products, and they are partially metabolites in nature. Moreover, these antibiotic wastes are reported to be bioaccumulated, bio-transformed, and deposited in the solid and aqueous phases [7], thus increased the antibiotic persistence in the environment.

A fluoroquinolone antibiotic called ofloxacin (OFL) has been utilized for treating bacterial infections of the skin, lungs, and urinary tract [8]. Fluoroquinolones may be discovered in amounts ranging from 18.28 ng L^{-1} to 6,058 µg L^{-1} in hospital, wastewater, and slaughterhouse effluent. These range of values exceeded the values recommended by The World Health Organization (WHO) guideline that should be less than 100 µg L^{-1}. Although several reports claimed that the measured concentration of ofloxacin in water bodies is lower than the limit, its presence is still a severe problem that should be eliminated. Researchers have been working on developing methods to eradicate this contaminant using adsorption [9], biosorption [10], or photocatalysis [11] methods. Nonetheless, photocatalysis remains as one of the best strategies for antibiotic degradation as it is cost-effective and generates little waste. Conventional photocatalysts, such as TiO_2 and ZnO, have significant drawbacks, including a restricted response to visible light irradiation as a result of their large band gap energies of 3.2 eV and 3.3 eV, respectively [12,13]. As a result, research on alternatives has been conducted to overcome the restrictions.

Soltani et al. [14] discovered that bismuth ferrite ($BiFeO_3$) has a band gap of 2.17 eV, which is narrow and is theoretically suitable for the operation employing visible light irradiation. $BiFeO_3$ enhanced magnetic and optical characteristics, as well as its increased oxidizing capacity, has made it a viable photocatalyst [15]. This material exists in three common phases: perovskite ($BiFeO_3$), mullite ($Bi_2Fe_4O_9$), and sillenite ($Bi_{25}FeO_{40}$), each with slightly different photocatalytic performance [16]. Previously, Yang et al. [17] used a sillenite phase of $BiFeO_3$ in the degradation of levofloxacin, and the photocatalytic activity was exceptional. Zahra et al. [18] also employed $BiFeO_3$ for tetracycline breakdown and demonstrated substantial potential under visible light irradiation.

The initial concentration of pollutants, photocatalyst dosage, pH solution, and irradiation time are examples of the important operational parameters in the photocatalytic reaction. As Wang et al. [19] reported, the removal efficiency increases with increasing catalyst dosage until it reaches the optimum dosage and start to decline as the dosage further increase. The turbidity of the solution caused the reduction in the photon penetration through the solution. In their work, Hapeshi et al. [20] stated that the removal efficiency of ofloxacin started to decrease from 100 % to 88 % as the initial concentration increased from 10 mg L^{-1} to 20 mg L^{-1}. Besides, Hu et al. [16] also reported that the solution pH could affect the photocatalytic degradation of bisphenol A due to the alteration of the surface charge in different pH conditions.

The morphological, optical, and other features of the produced perovskite $BiFeO_3$ were studied in this work. Also, the influence of the operating settings on the ofloxacin photocatalytic degradation by $BiFeO_3$ was investigated under the illumination of sunlight.

Materials and Methods

Bismuth nitrate pentahydrate ($Bi(NO_3)_3.5H_2O$), iron nanohydrate ($Fe(NO_3)_3.9H_2O$), *kappa*-carrageenan, and ofloxacin were all purchased from Sigma-Aldrich with more than 99 % purity. Meanwhile, sodium hydroxide (NaOH) pellets, sodium nitrate ($NaNO_3$), ethanol (99.7%), and hydrochloric acid (HCl) (37%) were supplied from R&M Chemicals.

Synthesis of perovskite bismuth ferrite (BFO)

$BiFeO_3$ nanoparticles were synthesised utilising the sol-gel technique with bio-templating, as proposed by Satar et al. [21]. An amount 2.80 g bismuth nitrate pentahydrate ($Bi(NO_3)_3.5H_2O$) was first dissolved in 50 mL deionized water. The aforementioned solution was then mixed with 4.04 g of iron (III) nitrate nonahydrate ($Fe (NO_3)_3.9H_2O$). In 100 mL of deionized water, 1.00 g of *kappa*-carrageenan powder (1%) was dissolved completely. Following that, 40 mL of 1%-carrageenan solution and 10 mL of Bi and Fe salts solution were mixed and agitated with a magnetic stirrer. Using 1.0 M NaOH solution, the pH of the combination was adjusted to pH 10. The resultant sol was dried in an oven at 80 °C overnight after 2 hours of stirring. In the muffle furnace, the dried gel was calcined for 2 hours at 550 °C. Subsequently, the powder was rinsed multiple times with deionized water and ethanol prior drying at 80 °C for 2 hours.

Characterization of perovskite bismuth ferrite (BFO)

The X-Ray Diffraction (XRD) pattern of $BiFeO_3$ nanoparticles was obtained using a PANalytical X'Pert PRO with graphite monochromator and Cu K radiation ($\lambda = 1.5406$) in the range of 10 - 80°. The morphology and chemical composition of $BiFeO_3$ nanoparticles before and after photocatalytic activity were examined utilizing scanning electron microscopy (SEM, FEI-QUANTA FEG 650) and an Energy Dispersive X-Ray spectroscopy (EDX) microanalyzer (INCA X, Oxford Instruments). The band gap of $BiFeO_3$ was estimated using the reflectance percentage (%R) acquired from the UV-vis diffraction reflectance (UV-DRS) spectrophotometer (LAMBDA 25). The functional group present in $BiFeO_3$ was identified using Perkin Elmer's System 2000 IR in the wavenumber range 4000 – 400 cm^{-1}. Through nitrogen adsorption (BET analyser), the surface features and porosity of $BiFeO_3$ were investigated using the Micromeritics ASAP 2020 Surface Area and Porosity analyzer. Finally, the removal of total organic carbon (TOC) was assessed using a TOC analyzer (Shimadzu TOC-L).

Degradation of ofloxacin under direct sunlight

The photocatalytic activities of $BiFeO_3$ nanoparticles were investigated using the degradation of ofloxacin (OFL) solution in the presence of sunlight. This study was carried out between March and August 2021, from 11 a.m. to 3 p.m. Typically, 100 mL of 10 mg L^{-1} OFL solution (unadjusted pH) was placed into a beaker followed by adding catalyst (10 mg, that corresponds to 0.1 g L^{-1}). First, the solution was magnetically agitated for 30 minutes in the dark to produce adsorption-desorption equilibrium. The solution was then exposed to sunlight for 2 hours. Sampling was performed by withdrawing 5 mL of the solution at 20-minute intervals and filtering with 0.22-micron filters before been analyzed at 288 nm using UV-vis spectrophotometer (Shimadzu UV-2600). A control experiment was done by using the same procedure but without the presence of photocatalyst. A calculation by using the following equation was made to obtain the percentage removal of OFL solution:

$$Removal\ (\%) = \left(1 - \frac{C_t}{C_o}\right) \times 100 \qquad (1)$$

Based on the above equation, removal (%) represents the percentage removal of OFL in the experiments. C_t and C_o represent the concentration of OFL at the given time and the initial concentration of OFL, respectively. The effect of catalyst dosage in the experiment was carried out by varying the dosage at 0.05, 0.07, 0.09, 0.3, and 0.5 g L^{-1}. For the effect of pH, 0.1 M NaOH and 0.1 M HCl were used to alter the pH to obtain pH 2, 4, 6, 8, 10, and 12. In the initial concentration of the OFL solution, the concentration used are 2.5, 5, 10, 15, and 20 mg L^{-1} and finally, 0.1, 0.3, 0.5, and 0.7 M H_2O_2 were used to study the effect of hydrogen peroxide in the photocatalytic degradation OFL by $BiFeO_3$ photocatalyst. For each parameter, the test was repeated thrice to achieve an average value.

Results and discussion

Structural and morphological analysis of $BiFeO_3$

$BiFeO_3$ had been successfully synthesized by using the sol-gel method with kappa-carrageenan as a bio template as shown in Figure 1. The chains of κ-carrageenan performed cross-linking to give the protective layers and stabilize the Fe^{3+} and Bi^{3+} ions. As the pH of the mixture increases, κ-carrageenan self-capped the ions and this localized area became the nucleation and growth sites of the $BiFeO_3$ particles. The calcination process did the elimination of κ-carrageenan and the structure of $BiFeO_3$ remained. Figure 2 depicts SEM micrographs and EDX spectra of $BiFeO_3$ nanoparticles before and after photocatalytic degradation. Figure 2(a) shows the morphology of unused $BiFeO_3$ as distorted rhombohedral structure and homogeneously distributed. The average particle size calculated by J-image software, is 90 nm as in agreement with previous method. The SEM micrograph for the employed $BiFeO_3$ in Figure 2(b) confirmed that no substantial changes could be noticed, although average particle sizes increase to more or less than 170 nm. This could be due to $BiFeO_3$ agglomeration after being utilized in photocatalytic activity. The presence of elements such as Bi, Fe, and O in the sample was demonstrated by EDX and the absence of additional elements verified the samples purity. The XRD pattern of synthesized $BiFeO_3$ was demonstrated in Figure 3(a). The catalyst exhibited diffraction peaks at 2θ = 22.48°, 32.12°, 39.56°, 45.89°, 51.67°, 57.12°, and 67.18°, which corresponded to pure rhombohedral phase $BiFeO_3$ Miller's indices of (0 1 2), (1 1 0), (0 2 4), (1 1 6), (3 0 0), and (2 2 0). This pattern is in agreement to the standard perovskite $BiFeO_3$ data (JCPDS card No. 01-073-0548). The predominant peak that could be assigned was (1 0 1), and no corresponding impurity peak was observed, implying that the $BiFeO_3$ nanoparticles produced were pure and exhibited a highly crystalline distorted rhombohedral structure.

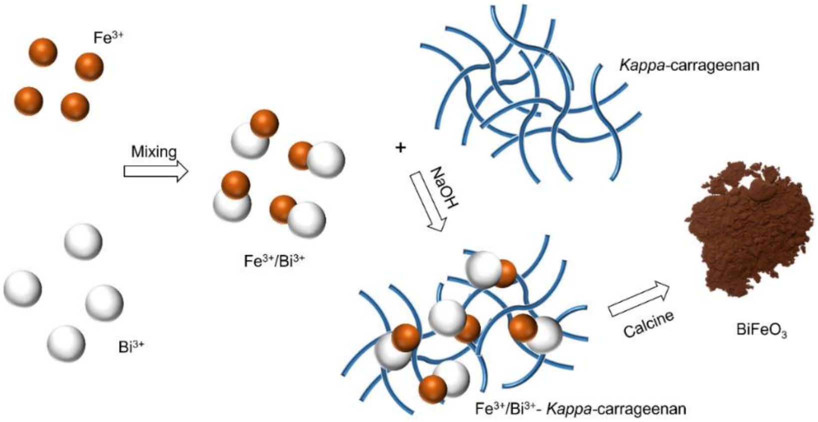

Figure 1. The possible mechanism of utilization of κ-carrageenan as the biotemplate in the synthesis of $BiFeO_3$ nanoparticles

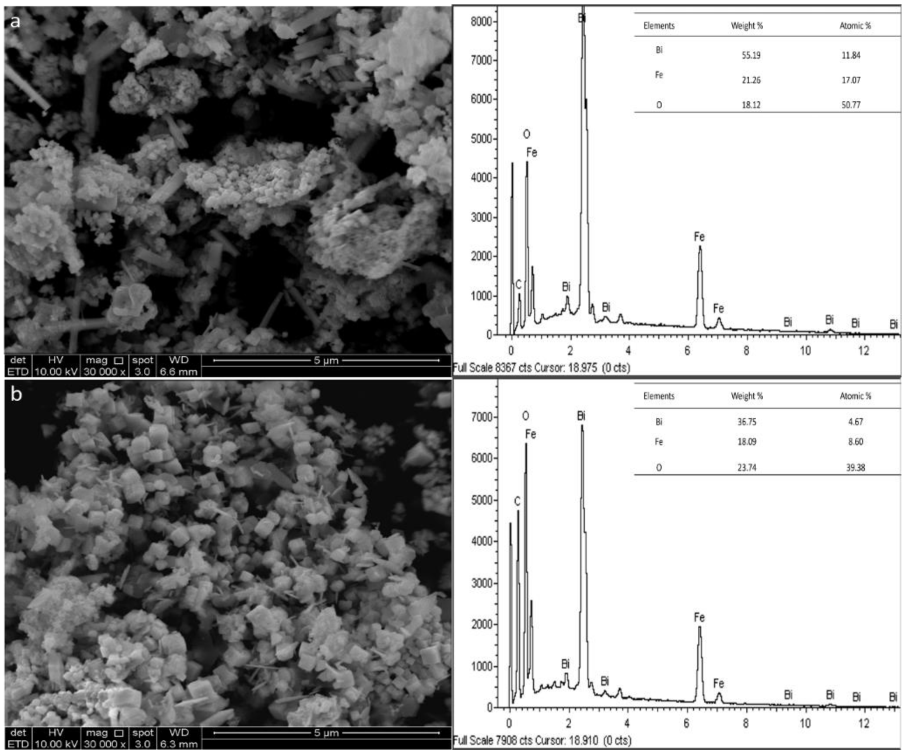

Elements	Weight %	Atomic %
Bi	55.19	11.84
Fe	21.26	17.07
O	18.12	50.77

Elements	Weight %	Atomic %
Bi	36.75	4.67
Fe	18.09	8.60
O	23.74	39.38

Figure 2. The SEM images of (a) $BiFeO_3$ photocatalyst, and (b) $BiFeO_3$ photocatalyst (used) and their elemental composition

Analysis of the N_2 sorption isotherm

Brunauer, Emmett, and Teller (BET) nitrogen adsorption analysis was used to determine the N_2 sorption isotherm, pore size, pore volume and surface area of $BiFeO_3$. Based on Figure 3(b), the isotherm obtained suggested that $BiFeO_3$ has Type IV and H3 hysteresis loop classification, implying that the sample was primarily composed of mesopores [22] typically range from 2 nm to 50 nm. The presence of plate-like particles in the sample, which aggregated to create slit-shaped pores, is indicated by the H3 hysteresis loop [23]. Figure 3(c) displays pore distribution model (PSD) based on Barrett-Joyner-Halenda (BJH) theory, with pore diameters ranging from 8 nm to 98 nm, confirming the material has mesoporous pores. The PSD plot demonstrated that the pore size and pore volume of $BiFeO_3$ were 31.94 nm and 0.041 $cm^3\ g^{-1}$, respectively, and the surface area obtained was 4.67 $m^2\ g^{-1}$. The porosity features are essential because they can be associated with the adsorption-desorption process of pollutant molecules to the photocatalyst prior to degradation by the photocatalysis process.

BFO optical analysis

The photocatalyst optical properties aid in determining their band gap energy, which is connected to the UV-absorption edge. The UV-vis diffraction reflectance spectra of the synthesized $BiFeO_3$ photocatalyst are depicted in Figure 3(d), and it exhibits substantial absorption of light in the visible light spectrum. Kubelka-Munk theory formula was used to determine the band gap energy of $BiFeO_3$. The corresponding band gap energy can be ascertained from the extrapolated tangent line in the plot of squared Kubelka-Munk functions, $F(R)^2$ vs photon energy of $E=h\nu$. The band gap energy obtained for the as-prepared $BiFeO_3$ is 2.04 eV, which is less than 2.10 eV found in previous investigations by Huo et al. [24]. The decrease in band gap energy could be caused by the lattice strain effect in $BiFeO_3$, which is correlated to particle size reduction. As a result, $BiFeO_3$ nanoparticles were demonstrated to be responsive to visible light and can be employed for the photodegradation of contaminants under visible light.

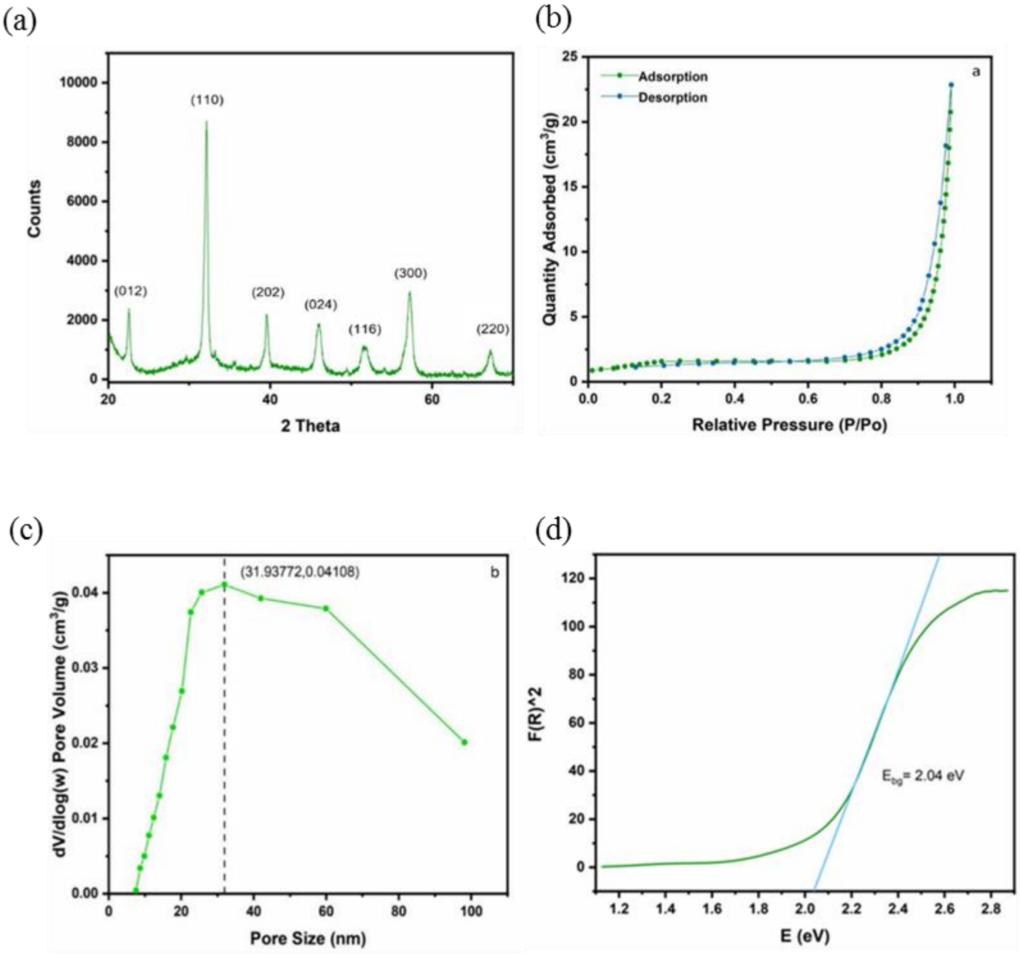

Figure 3. The (a) XRD pattern, (b) nitrogen linear adsorption, (c) pore size distribution and (d) bandgap energy of synthesized $BiFeO_3$ nanoparticles

BFO FTIR spectra

FT-IR spectroscopy analysis was utilized to validate the presence of functional groups in the synthesized perovskite $BiFeO_3$. Figure 4(a) reveals a broad and strong absorption band between 3000 cm^{-1} and 3500 cm^{-1} that can be referred to as stretching vibrations of the O-H group, while the bending vibrations mode of water can be detected at 1625 cm^{-1}. Bending vibrations of Fe-O and Bi-O may be observed at the sharp peak at 568 cm^{-1} and 457 cm^{-1}, respectively. These absorptions corresponded to the features of the octahedral FeO_6 group found in perovskite compounds like $BiFeO_3$.

Figure 4(b) depicts the FTIR spectrum of $BiFeO_3$ employed in the photocatalytic degradation of ofloxacin. There were slight changes observed, such as the shape of stretching vibrations of O-H group to a medium broad absorption band and the loss of nitrate groups at 875 cm^{-1}. However, some absorption bands, particularly the Fe-O and Bi-O bending vibrations of $BiFeO_3$ nanoparticles, were successfully preserved. As a result, this proves that $BiFeO_3$ is a stable catalyst that is not damaged by the contaminants.

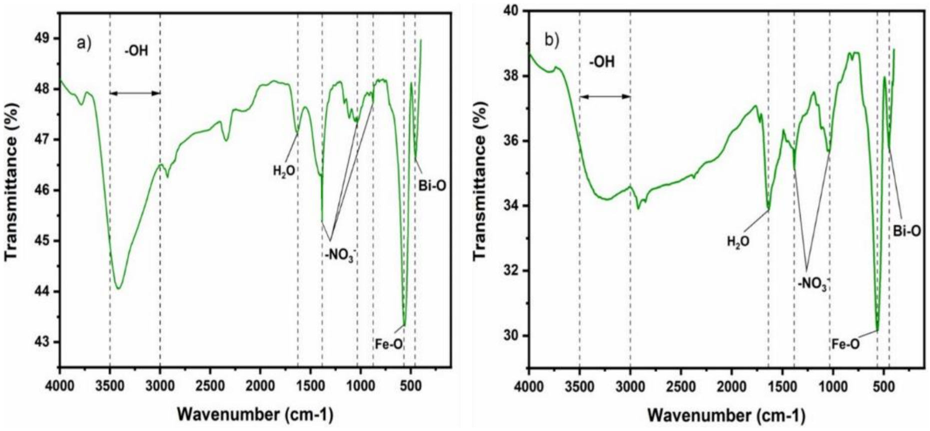

Figure 4. FTIR spectra of $BiFeO_3$ (a) before and (b) after photocatalytic reactions

Point of zero charge (PZC)

At a specific pH level, the point of zero charge (PZC) is a state in which there is no net charge on the surface of the molecules [25]. As illustrated in Figure 5(a), the point of zero charge (pH_{pzc}) pH value can be detected at the x-intercept of the plotted curve between the difference of final and initial pH and initial pH of the solution. $BiFeO_3$ pH_{pzc} value was 7.75, which is in the neutral region. When the pH value was less than pH_{pzc}, the presence of the positive charge on the surface of the $BiFeO_3$ can be observed. Whereas, at the pH value above pH_{pzc}, the presence of negative charge can be observed on the surface of the photocatalyst. The electrostatic interaction between the photocatalyst and pollutant molecules can be linked to the effect of pH on the photodegradation efficiency of $BiFeO_3$.

Degradation of ofloxacin by photocatalysis: Catalyst dosage

The degradation of ofloxacin in the control experiment gave a non-significance result, thus the research was continued with the operational parameter studies. The influence of catalyst dosage was studied by changing the $BiFeO_3$ dosage from 0.05 g L^{-1} to 0.50 g L^{-1} in a solution of 20 mg L^{-1} of ofloxacin without adjusting the pH level. This investigation is necessary to ascertain the best amount of catalyst to be utilized in order to maximize the photocatalyst's potential. Table 1 and Figure 5(b) illustrate the effect, which were tabulated and plotted respectively. As the dosage increased from 0.05 g L^{-1} to 0.07 g L^{-1}, the degradation efficiency of $BiFeO_3$ was raised from 29.32 % to 34.96 %. The behaviour can be elucidated by the fact that as the catalyst dosage increases, the number of active sites in the photocatalyst increases, which is closely proportional to the number of radicals produced during the degradation of ofloxacin [26]. However, as the catalyst dosage is continuously increased from 0.09 g L^{-1} to 0.50 g L^{-1}, the degrading performance began to decline from 32.93 % to 23.47 %. When the amount of catalyst used exceeded the optimum dose, the turbidity of the solution increased, and photocatalyst particle agglomeration occurred in the solution, affecting the light penetration and reducing the photocatalytic activity of $BiFeO_3$ [14]. Photooxidation kinetics of ofloxacin depended on $BiFeO_3$ loading and it was discovered that the rates increased as the $BiFeO_3$ loading increased until a certain limit and then the rates started to decrease back to a constant value. Therefore, an optimum $BiFeO_3$ dosage added is important to prevent the unnecessary excess catalyst and to ensure total absorption of light photons for efficient photo mineralization. According to the findings, the best catalyst dosage in the experiment was 0.07 g L^{-1}, with a removal rate of 35% in 120 minutes under sunshine exposure.

Table 1. The removal efficiency of OFL at different $BiFeO_3$ dosage with respect to time. (Condition: 20 mg L^{-1} OFL with unadjusted pH and 120 min irradiation under sunlight)

BFO Dosage (g L^{-1})	**% Removal of OFL**		
	Dark (30 mins)	**1 hour**	**2 hours**
0.05	0.32	14.21	29.32
0.07	0.26	14.87	34.96
0.09	0.65	17.82	32.93
0.30	3.20	18.08	31.70
0.50	2.56	11.16	23.47

The pH of the ofloxacin solution

The photocatalytic activity of the photocatalyst has been found to be directly connected to the pH of the pollutants, which has an important influence on the degradation performance. The pH change may modify the electrical double layer of the catalyst and pollutant interface, affecting the adsorption-desorption processes and the separation of the carrier charges in catalyst particles. Ofloxacin, according to Crespo-Alonso et al. [27], is an amphoteric molecule that exists as an anion at pKa 8.22 and a cation at pKa 6.05 while exists as a zwitterion between these pKa values. The pH value of the 20 mg L^{-1} ofloxacin solution with a catalyst dosage of 0.07 g L^{-1} was done by adjusting the pH of solution from pH 2 to pH 12. The removal efficiency of ofloxacin increases from 16.84 % to 36.70 % as the pH decreases from 12 to 8, as tabulated in Table 2 and plotted in Figure 5(c). Then, as the pH value dropped to 6, the performance declined to 21.01 %. As the $BiFeO_3$ is within the acidic region at pH 2, its photocatalytic performance decreases significantly, with a very low value of 0.84 %. This suggests that the breakdown of ofloxacin in the acidic medium is unfavourable. At pH 2 and pH 4, the surface charge of $BiFeO_3$ is positive, and ofloxacin exists as a cation at these pH levels. As a result, electrostatic repulsion between the photocatalyst and pollutant molecules arises, resulting in a decrease in degradation efficiency. Nevertheless, the photocatalytic performances also declined in the strong alkaline region as the surface charge of $BiFeO_3$ is negative and ofloxacin exists in its anionic state as its structure undergoes deprotonation, which caused the repulsion between ofloxacin and $BiFeO_3$ molecules. These suggest that the breakdown of ofloxacin in the strong acidic and alkaline medium are unfavourable [28]. Therefore, the optimum pH value was obtained at pH 8 as the removal effectiveness was the highest, with 36.70 % removal. The $BiFeO_3$ surface exhibited anionic behaviour at pH 8, and ofloxacin occurred in a zwitterionic state with both positive and negative charges. As a result, electrostatic interaction between the $BiFeO_3$ surface and ofloxacin molecules might occur, thereby improving the removal efficiency of the antibiotic. The study proved that pH value variation could affect the adsorption of ofloxacin on the surface of $BiFeO_3$ and its photodegradation efficiency.

Table 2. The removal efficiency of OFL at different pH with respect to time(Condition: 0.07 g L^{-1} $BiFeO_3$, 20 mg L^{-1} OFL and 120 min irradiation under sunlight)

Solution pH	**% Removal of OFL**		
	Dark (30 mins)	**1 hour**	**2 hours**
2	0.14	2.82	0.84
4	3.35	4.59	3.79
6	1.58	11.05	21.01
8	5.93	22.10	36.70
10	1.24	16.59	29.19
12	9.89	13.63	16.84

Initial concentration of ofloxacin solution

The initial concentration study was done by using different concentrations of ofloxacin from 2.5 mg L^{-1} to 20 mg L^{-1} with the 0.07 g L^{-1} catalyst dosage and in pH 8 medium. Generally, the initial concentration study was conducted to identify the optimum concentration for the photocatalyst to carry out the photocatalysis optimally. Table 3 and Figure 5(d) show that as the initial concentration of ofloxacin increases from 2.5 mg L^{-1} to 10 mg L^{-1}, the degradation efficiency of ofloxacin also increases steadily from 37.00 % to 46.13 %. The optimum initial concentration in the study was 10 mg L^{-1} due to the highest removal efficiency. The removal efficiency decreased to 37.52 % and 36.78 %, respectively, when the starting concentration rose to 15 mg L^{-1} and 20 mg L^{-1}. This can be explained as the higher the concentration of ofloxacin, the higher the number of ofloxacin molecules in the medium. Therefore, a greater amount of light being absorbed by the ofloxacin molecules and reduced the photo flux from hitting the photocatalyst surface. Besides, the competition between the ofloxacin molecules might increase because of higher amount of pollutant molecules compared to the amount of available active sites on the photocatalyst [29]. It may be deduced that a high initial concentration of ofloxacin will reduce its removal effectiveness.

Table 3. The removal efficiency of OFL at different initial concentration with respect to time. (Condition: 0.07 g L^{-1} $BiFeO_3$, OFL solutions with pH 8 and 120-min irradiation under sunlight)

Concentration OFL (mg L^{-1})	**% Removal of OFL**		
	Dark (30 mins)	**1 hour**	**2 hours**
2.5	1.72	30.77	37.00
5.0	6.40	27.34	41.79
10.0	6.10	30.14	46.13
15.0	5.03	22.54	37.52
20.0	5.42	22.44	36.78

Effect of hydrogen peroxide addition

The final parameter in this work is the influence of the addition of hydrogen peroxide (H_2O_2) to the extent of the photocatalysis reaction. The study on the effect of H_2O_2 addition was carried out by adding a different concentration of H_2O_2 from 0.1 M to 0.7 M in 10 mg L^{-1} of ofloxacin solution at a pH level of 8 with 0.07 g L^{-1} catalyst dosage. As shown in Table 4 and Figure 5(e), the removal efficiency drastically increases as the concentration of hydrogen peroxide introduced increases from 0.1 M to 0.3 M with an efficiency of 56.68 % to 70.10%, respectively. However, as the concentration of H_2O_2 kept on increasing, only a small amount of increment can be observed in the removal efficiency being the highest of 72.42 % with 0.7 M of H_2O_2. The trend that can be seen from the study may cause by the increased number of radicals generated from the breakdown of hydrogen peroxide through the reduction of it at the conduction band and decomposition by the illumination of sunlight. As the concentration of H_2O_2 increases beyond 0.3 M, the generation of radicals may achieve saturation as the removal efficiency only slightly increases. The purpose of this study was to utilize the lowest possible concentration of H_2O_2 used with excellent removal efficiency as in low concentrations of H_2O_2, more efficient is the production of hydroxyl radicals and inhibition of charge carrier recombination. Besides, the solution may sometimes experience oxygen starvation because of slow oxygen mass transfer or oxygen consumption. The addition of H_2O_2 can help to achieve a sufficient oxygen supply and modify the $BiFeO_3$ surface, however high concentration of it could act as photoproduced holes scavenger. Therefore, the optimum concentration of H_2O_2 used in the study was 0.3 M. The results proved that the introduction of hydrogen peroxide with minimal concentration could successfully boost the photocatalytic degradation of ofloxacin by $BiFeO_3$.

Table 4. The removal efficiency of OFL at different concentration H_2O_2 used with respect to time. (Condition: 0.07 g L^{-1} $BiFeO_3$, 10 mg L^{-1} OFL with pH 8 and 120-min irradiation under sunlight).

Concentration H_2O_2 (M)	**% Removal of OFL**		
	Dark (30 mins)	**1 hour**	**2 hours**
0.1	13.42	44.75	56.68
0.3	7.46	31.32	70.10
0.5	13.04	59.39	70.97
0.7	10.14	59.39	72.42

Kinetic model and total organic carbon (TOC) removal

The Langmuir-Hinshelwood (LH) model was used to investigate the reaction kinetics for the photocatalytic degradation of ofloxacin. The model has usually been utilized for the heterogeneous photocatalytic degradation in various types of pollutants and simplified to pseudo-first order expression [16]. Figure 5(f) shows the plotted LH model and the data obtained are tabulated in Table 5. The LH equation had been simplified into a pseudo-first order kinetic model equation as follows:

$$ln\frac{C_t}{C_o} = kt \qquad (2)$$

where, C_o and C_t are the initial concentration of ofloxacin and concentration of ofloxacin at the time, t, respectively. k is the degradation rate constant and t is the irradiation time. k value can be obtained directly from the slope of the plot between ln C_o/C_t versus irradiation time. Based on the plotted graph and its square of correlation coefficient (0.9399), r^2, it can be concluded that the reaction followed pseudo-first order kinetic and fitted the model perfectly and k value obtained from the graph was 0.0084 min^{-1}.

Next, total organic carbon (TOC) removal is an important study and can be used to identify the total carbon content of the organic pollution in the water bodies after being treated [30]. From the plot in Figure 6(a), after exposure to sunlight for 120 mins, 65.99% of ofloxacin has been degraded by $BiFeO_3$. On the contrary, as shown in Figure 6(b), the total organic content (TOC) in the solution has been significantly removed and left with only 9.36%. The great efficiency of mineralization shows that $BiFeO_3$ is an excellent photocatalyst to be applied in wastewater treatment.

Table 5. The rate constant and correlation factor of LH kinetic model for OFL antibiotic. (Condition: 0.07 g L^{-1} $BiFeO_3$, 0.3 M H_2O_2 added, 10 mg L^{-1} OFL with pH 8 and 120-min irradiation under sunlight)

	Langmuir- Hinshelwood Kinetic Model	
OFL	**K_{LH} (min^{-1})**	**R^2**
	0.0084	0.9399

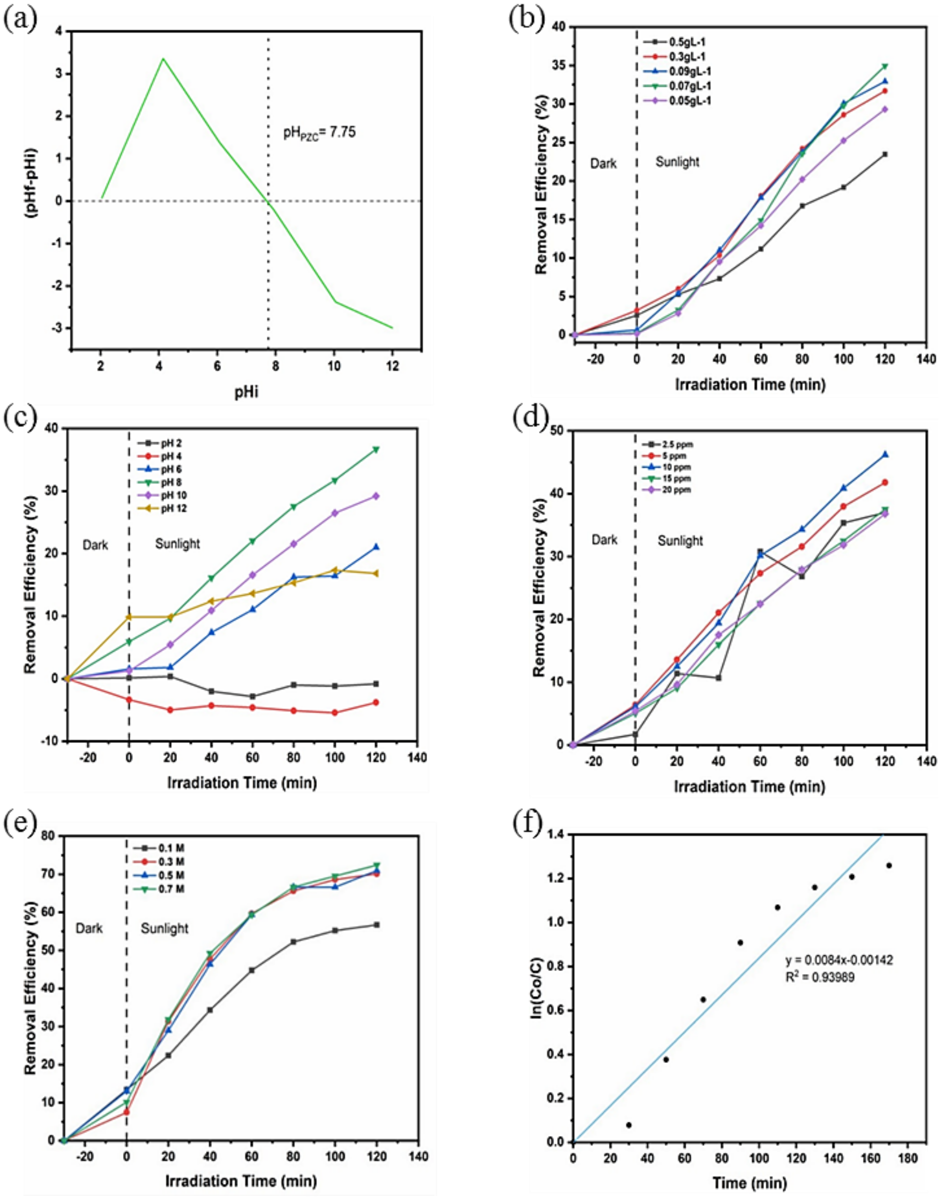

Figure 5. (a) pHpzc of $BiFeO_3$, the removal efficiency of OFL under different (b) $BiFeO_3$ dosage (c) pH of solution, (d) initial concentration (e) H_2O_2 model for OFL degradation using $BiFeO_3$ versus irradiation time and (f) Langmuir-Hinshelwood kinetic model

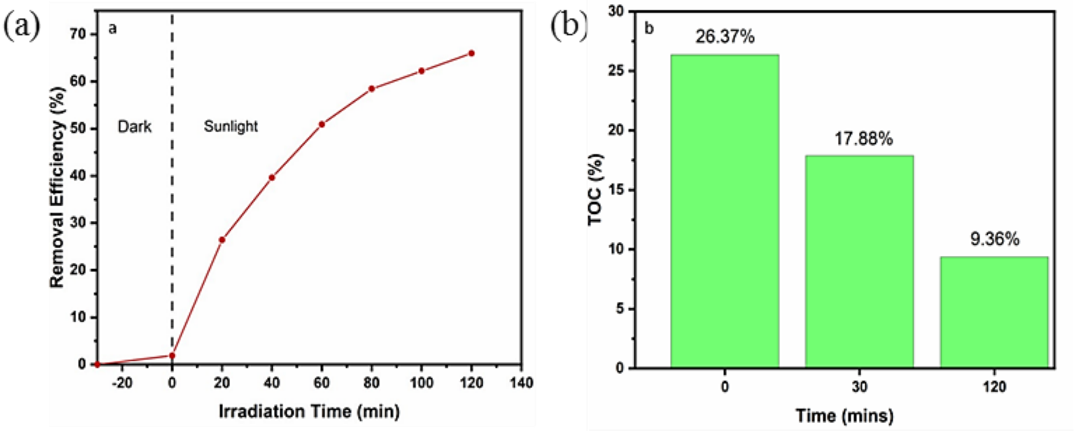

Figure 6. The (a) removal efficiency of OFL for TOC analysis and (b) depletion in TOC value of OFL solution with respect to time (Condition: 0.07 g L^{-1} $BiFeO_3$, 0.3 M H_2O_2 added, 10 mg L^{-1} OFL with pH 8 and 120-min irradiation under sunlight)

Conclusion

In conclusion, a facile $BiFeO_3$ photocatalyst was synthesized effectively using the bio-templated sol-gel approach. The purity of the photocatalyst, as well as significant chemical and physical properties, were investigated using various experimental characterizations. $BiFeO_3$ has been shown to have important properties, such as a narrow band gap energy of 2.04 eV with a surface area of 4.67 m^2 g^{-1}. Photocatalysis in the presence of $BiFeO_3$ has been proven to have an excellent property to eliminate ofloxacin with 70.1 % removal efficiency under optimum conditions. The effect of the parameters was controversial in some cases; thus, it is required to further study the nature of the pollutant to be degraded, and on types of photocatalyst to be utilized in the photodegradation. The kinetic study was conducted and found that the reaction is in good agreement with Langmuir-Hinshelwood kinetic model. The TOC analysis showed a great mineralization of ofloxacin. The knowledge of photocatalytic activity and its operational parameters could provide a better understanding for the elimination of pollutants, especially antibiotics.

Acknowledgement

The author gratefully acknowledges financial assistance from the Ministry of Higher Education (MOHE) under the Fundamental Research Grant Scheme (FRGS) [FRGS/1/2019/STG07/USM/02/7]. The author also acknowledges School of Chemical Sciences, Centre for Global Archaeological Research, School of Physics, USM and Nagaoka University of Technology, Japan for the research facilities.

Reference

1. Siddique, M., Khan, N. M., & Saeed, M. (2019). Photocatalytic activity of bismuth ferrite nanoparticles synthesized via sol-gel route. *Zeitschrift Fur Physikalische Chemie*, 233(5): 595-607.
2. Huang, Q., Liu, Y., Cai, T. and Xia, X. (2019). Simultaneous removal of heavy metal ions and organic pollutant by BiOBr/Ti3C2 nanocomposite. *Journal of Photochemistry and Photobiology A: Chemistry*, 375(December 2018): 201-208.
3. Boruah, P. K. and Das, M. R. (2020). Dual responsive magnetic Fe_3O_4-TiO_2/graphene nanocomposite as an artificial nanozyme for the colorimetric detection and photodegradation of pesticide in an aqueous medium. *Journal of Hazardous Materials*, 385: 121516.
4. Sharma, P., Kumar, N., Chauhan, R., Singh, V., Srivastava, V. C. and Bhatnagar, R. (2020). Growth of hierarchical ZnO nano flower on large functionalized rGO sheet for superior photocatalytic mineralization of antibiotic. *Chemical Engineering Journal*, 392: 123746.

5. Van Boeckel, T. P., Gandra, S., Ashok, A., Caudron, Q., Grenfell, B. T., Levin, S. A. and Laxminarayan, R. (2014). Global antibiotic consumption 2000 to 2010: An analysis of national pharmaceutical sales data. *The Lancet Infectious Diseases,* 14(8): 742-750.
6. Ambrosetti, B., Campanella, L. and Palmisano, R. (2015). Degradation of antibiotics in aqueous solution by photocatalytic process: Comparing the efficiency in the use of ZnO or TiO_2. *Journal of Environmental Science and Engineering A,* 4(6): 273-281.
7. Manzetti, S. and Ghisi, R. (2014). The environmental release and fate of antibiotics. *Marine Pollution Bulletin,* 79(1–2): 7-15.
8. Huang, J., Cao, J., Ding, Y., Hu, Y., Cen, Y. and Tang, H. (2018). Variable-valence metals catalyzed solid $NaBiO_3$ nanosheets for oxidative degradation of norfloxacin, ofloxacin and ciprofloxacin: Efficiency and mechanism. *Chemosphere,* 205: 531-539.
9. Wang, J., Tsuzuki, T., Tang, B., Hou, X., Sun, L. and Wang, X. (2012). Reduced graphene oxide/ZnO composite: Reusable adsorbent for pollutant management. *ACS Applied Materials and Interfaces, 4(6),* 3084-3090.
10. Nurchi, V. M., Crespo-Alonso, M., Pilo, M. I., Spano, N., Sanna, G. and Toniolo, R. (2019). Sorption of ofloxacin and chrysoidine by grape stalk. A representative case of biomass removal of emerging pollutants from wastewater. *Arabian Journal of Chemistry,* 12(7): 1141-1147.
11. Bhatia, V., Ray, A. K. and Dhir, A. (2016). Enhanced photocatalytic degradation of ofloxacin by co-doped titanium dioxide under solar irradiation. *Separation and Purification Technology*, 161: 1-7.
12. Dai, J. F., Xian, T., Di, L. J. and Yang, H. (2013). Preparation of $BiFeO_3$ -graphene nanocomposites and their enhanced photocatalytic activities. *Journal of Nanomaterials,* 2013: 1155.
13. Moussa, H., Girot, E., Mozet, K., Alem, H., Medjahdi, G. and Schneider, R. (2016). ZnO rods/reduced graphene oxide composites prepared via a solvothermal reaction for efficient sunlight-driven photocatalysis. *Applied Catalysis B: Environmental*, 185: 11-21.
14. Soltani, T. and Entezari, M. H. (2013). Photolysis and photocatalysis of methylene blue by ferrite bismuth nanoparticles under sunlight irradiation. *Journal of Molecular Catalysis A: Chemical*, 377(3): 197-203.
15. Gómez-Pastora, J., Dominguez, S., Bringas, E., Rivero, M. J., Ortiz, I. and Dionysiou, D. D. (2017). Review and perspectives on the use of magnetic nanophotocatalysts (MNPCs) in water treatment. *Chemical Engineering Journal*, 310: 407-427.
16. Hu, Z. T., Liu, J., Yan, X., Oh, W. Da and Lim, T. T. (2015). Low-temperature synthesis of graphene/$Bi_2Fe_4O_9$ composite for synergistic adsorption-photocatalytic degradation of hydrophobic pollutant under solar irradiation. *Chemical Engineering Journal,* 262: 1022-1032.
17. Liu, Y., Guo, H., Zhang, Y., Tang, W., Cheng, X. and Li, W. (2018). Heterogeneous activation of peroxymonosulfate by sillenite $Bi_{25}FeO_{40}$: Singlet oxygen generation and degradation for aquatic levofloxacin. *Chemical Engineering Journal,* 343(February): 128-137.
18. Rouhani, Z., Karimi-Sabet, J., Mehdipourghazi, M., Hadi, A. and Dastbaz, A. (2019). Response surface optimization of hydrothermal synthesis of Bismuth ferrite nanoparticles under supercritical water conditions: Application for photocatalytic degradation of Tetracycline. *Environmental Nanotechnology, Monitoring and Management,* 11: 100198.
19. Wang, X., Wan, X., Xu, X. and Chen X. (2014). Facile fabrication of highly efficient AgI/ZnO heterojunction and its application of methylene blue and rhodamine B solutions degradation under natural sunlight. *Applied Surface Sciences,* 321:10-8.
20. Hapeshi, E., Achilleos, A., Vasquez, M. I., Michael, C., Xekoukoulotakis, N. P., Mantzavinos, D. (2014). Drugs degrading photocatalytically: Kinetics and mechanisms of ofloxacin and atenolol removal on titania suspensions. *Water Research,* 44(6):1737-1746.

21. Satar, N. S. A., Aziz, A. W., Yaakob, M. K., Yahya, M. Z. A., Hassan, O. H., Kudin, T. I. T. and Kaus, N. H. M. (2016). Experimental and first-principles investigations of lattice strain effect on electronic and optical properties of biotemplated $BiFeO_3$ nanoparticles. *Journal of Physical Chemistry C,* 120(45): 26012-26020.
22. Lowell, S., Shields, J. E., Thomas., M. A. (2004). Characterization of porous solids and powders: surface area, pore size and density. *Molecularly Imprinted Materials: Science and Technology,* 127(40): 14118-14120.
23. Sing, K. S. W., Everett, D. H., Haul, R. A. W., Moscou, L., Pierotti, R. A., Rouquerol, J., & Siemieniewska, T. (1985). Reporting physisorption data for gas/solid systems with special reference to the determination of surface area and porosity. *Pure and Applied Chemistry,* 57(4): 603-619.
24. Huo, Y., Jin, Y. and Zhang, Y. (2010). Citric acid assisted solvothermal synthesis of $BiFeO_3$ microspheres with high visible-light photocatalytic activity. *Journal of Molecular Catalysis A: Chemical,* 331(1–2): 15-20.
25. Fiol, N. and Villaescusa, I. (2009). Determination of sorbent point zero charge: Usefulness in sorption studies. *Environmental Chemistry Letters,* 7(1): 79-84.
26. Xu, H. Y., Wu, L. C., Zhao, H., Jin, L. G. and Qi, S. Y. (2015). Synergic effect between adsorption and photocatalysis of metal-free g-C_3N_4 derived from different precursors. *PLoS One,* 10(11): 1-20.
27. Crespo-Alonso, M., Nurchi, V. M., Biesuz, R., Alberti, G., Spano, N., Pilo, M. I., & Sanna, G. (2013). Biomass against emerging pollution in wastewater: Ability of cork for the removal of ofloxacin from aqueous solutions at different pH. Journal of Environmental Chemical Engineering, 1(4), 1199–1204.
28. Peres, M. S., Maniero, M. G. and Guimarães, J. R. (2015). Photocatalytic degradation of ofloxacin and evaluation of the residual antimicrobial activity. *Photochemical Photobiological Sciences*;14(3):556-562.
29. Senasu, T., Chankhanittha, T., Hemavibool, K. and Nanan, S. (2021). Visible-light-responsive photocatalyst based on ZnO/CdS nanocomposite for photodegradation of reactive red azo dye and ofloxacin antibiotic. *Materials Science in Semiconductor Processing,* 123: 105558.
30. Lescano, M. R., Lopez, A. O., Romero, R. L. and Zalazar, C. S. (2021). Degradation of chlorpyrifos formulation in water by the UV/H_2O_2 process: Lumped kinetic modelling of total organic carbon removal. *Journal of Photochemistry and Photobiology A: Chemistry,* 404: 112924.